Journal of Chromatography, 598 (1992) 115–121
Elsevier Science Publishers B.V., Amsterdam

CHROM. 24 017

Fluorescence detector cell for use in an integrated electrically driven separation system

P. K. de Bokx*, E. E. A. Gillissen, P. van de Weijer, M. H. J. Bekkers and C. H. M. van Bommel

Philips Research Laboratories, P.O. Box 80 000, 5600 JA Eindhoven (Netherlands)

H.-G. Janssen

Eindhoven University of Technology, P.O. Box 513, 5600 MB Eindhoven (Netherlands)

(First received September 3rd, 1991; revised manuscript received January 27th, 1992)

ABSTRACT

An integrated design for electrically driven separations is presented. The injector, column and detector are all located within the same cartridge, allowing for integral thermostating and short column lengths. Results on the performance of the proposed fluorescence detector are reported. Molar amounts as low as $2 \cdot 10^{-19}$ mol of fluorescein (100-pl detector cell volume) can be detected. Short column lengths permit very fast separations, as is demonstrated by the separation of four laser dyes within 35 s.

INTRODUCTION

Electrically driven separation methods, including capillary zone electrophoresis (CZE) [1–3], micellar electrokinetic chromatography [4,5] and electrochromatography [6,7], are currently attracting a great deal of attention. Their common characteristic is that the flow through the "separation column" is effected by electroosmosis rather than by a pressure gradient. There are two main analytical reasons for such interest: first, superior separation efficiencies can be attained, with plate counts an order of magnitude higher than are possible in traditional liquid chromatography, and second, extremely small sample volumes can be handled. Depending on the inner diameter of the separation capillary, injection volumes can range from several tens of picolitres to the low nanolitres level, creating possibilities for single-cell sampling in the biological sciences [8] and local dissolution and sampling in materials research.

Owing to their common characteristics, many of the operating parameters (*e.g.*, field strength, buffer concentration, column diameter, column length) affect the separation performance of all electrically driven separation techniques in a similar fashion. As is outlined in the Theory section, there is a great deal to be gained with respect to efficiency and, more important, time of analysis (seconds rather than minutes) if high field strengths and short column lengths can be employed. In the present generation of instruments, short column lengths cannot be used owing to the physical distance that has to be spanned between the injector and detector. At a given maximum voltage of the power supply, this also limits the attainable field strength. Moreover, high field strengths require active thermostating to dissipate efficiently the Joule heat generated by the current. To benefit from the prospects offered by high field strengths and short column lengths, a new instrument concept is called for that takes into account the stringent requirements placed on injector and detector volumes, and, at the same time, allows for integral thermostating. Such an integrated instrument design is presented under Experimental.

0021-9673/92/$05.00

In this paper, we report on the detector cell of the instrument. Owing to the very small detector cell volumes required, the use of several widely employed detection principles, *e.g.*, UV absorbance detection and refractive index detection, is precluded. Detection should be based on phenomena of high inherent sensitivity. Fluorescence and electrochemical detection are the only likely candidates at present. Unfortunately, both methods are highly specific. In order to increase the versatility, one can either turn to derivatization or to indirect detection (adding a detectable compound to the eluent and measuring the decrease is signal due to presence of a solute [9]). Here, we demonstrate the use of a detector cell for fluorescence detection that is compatible with short column lengths and high field strengths and also adheres to the limitations placed on the maximum allowable detector cell volume.

THEORY

In this section, we investigate the separation properties of electrically driven systems. Our main aim is to show how the different operating parameters influence the separation performance with regard to efficiency and speed of analysis and to estimate how large the detector cell volume can be before a significant loss in this performance is observed.

The standard deviation of a chromatographic peak can be expressed in volume units as [10]

$$\sigma_{V,E} = (\pi/4)H\epsilon d_c^2\sqrt{N} \tag{1}$$

where H is the plate height, ϵ the void fraction (different from unity in the case of packed column electrochromatography), d_c the column diameter and N the plate number. The above standard deviation is a measure of the dispersion due to the column. We now demand that external contributions to the total dispersion do not seriously deteriorate the performance of the instrument. Following Naish *et al.* [11], we use as a criterion that the extra-column contribution to the total standard deviation should be less than half the dispersion caused by the column. Assigning half of the external dispersion to the detector and half to the injector and other sources, the maximum allowable detector cell volume can be obtained from

$$V_{DET} \leqslant \sqrt{\kappa} \cdot \frac{\sigma_{V,E}}{2\sqrt{2}} \tag{2}$$

where κ is the detection profile factor [12].

To make eqns. 1 and 2 explicit, we need an expression for the plate height of the peak. It is here, of course, that the specific characteristics of electrically driven separation techniques will become apparent. The great advantage of electrically driven systems is to be found in the plug profile of electroosmotic flow (for a detailed account, see Rice and Whitehead [13]). As there now is no tendency for the solute to be dispersed by radial differences in flow, one expects the only term to remain in the equation for the plate height of a solute that does not participate in any mass-transfer process to be that due to axial diffusion. Hence,

$$H = \frac{2\gamma D_m}{u} \tag{3}$$

where γ is the tortuosity factor, which is different from unity in the case of a packed bed, and D_m is the diffusivity of the solute. In electrically driven systems the linear velocity is given by the von Smoluchowski equation, $u = \varepsilon_r\varepsilon_0\zeta E/\eta$, where ε_0 and ε_r are the permittivity of free space and the relative permittivity, respectively, ζ (the zeta potential) is the potential at the plane of shear, E is the electric field strength and η is the viscosity. Substituting for u in eqn. 3 leads to

$$H = \frac{2\eta\gamma D_m}{\varepsilon_r\varepsilon_0\zeta} \cdot \frac{1}{E} \tag{4}$$

As noted by several workers [7,14], eqn. 4 is a simplification. Owing to self-heating of the eluent, a temperature gradient between the centre of the separation capillary and its walls will build up. Knox and Grant [7] calculated the excess temperature at the centre of the capillary, assuming the wall temperature to be constant. The resulting additional dispersion term is derived to be equal to

$$H = \frac{7 \cdot 10^{-9} \cdot \varepsilon_r\varepsilon_0\zeta\lambda^2\epsilon^2 d_c^6 c^2}{D_m\eta K^2} \cdot E^5 \tag{5}$$

where λ is the equivalent conductivity, c is the molar concentration of the eluent and K is its thermal conductivity.

Eqn. 5 indicates that this additional dispersion

term becomes particularly manifest at large column diameters and high field strengths. The total plate height, *i.e.*, the sum of eqns. 4 and 5, is plotted against field strength in Fig. 1 for three different column diameters.

Typical values used in the calculations are collected in Table I. The data clearly illustrate the need for small column diameters. Owing to self-heating, a diameter of 500 μm offers a working range that is extremely limited in voltage. Generally, a diameter of around 100 μm is accepted as a practical upper limit.

Key numerical results are collected in Table II, with values for the elution time of the electroosmotic peak, $t_E = L\eta/\varepsilon_r\varepsilon_0\zeta E$, the analysis time, t_A, assuming the slowest component to have a capacity factor of 10, the standard deviation of the unretained peak, $\sigma_{V,0}$, in volume units (eqn. 1), using eqns. 4 and 5, and the maximum allowable cell volume, V_{DET} (eqn. 2). Values were calculated for two column diameters, 100 and 50 μm. All calculations were performed at the minimum of the *H–E* curves (values for H_{min} and E_{opt} are indicated in the table title. The corresponding flows for 100- and 50-μm columns are 17.5 and 8.8 nls^{-1}, respectively.

It should be realized that the results in Table II were obtained based on the velocity of the electroosmotic peak (which is necessarily the fastest peak in electrochromatography) and using the values for the physical constants collected in Table I. Notwithstanding these constraints, several very interesting conclusions can be drawn from the results in Fig. 1

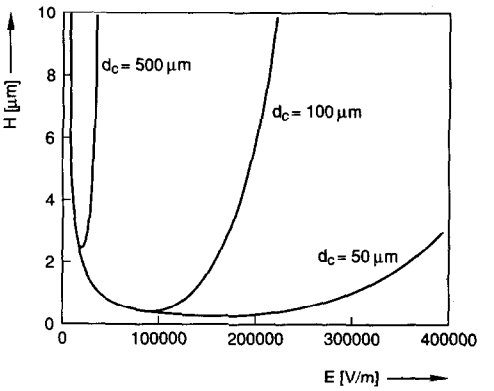

Fig. 1. Plots of total plate height (sum of eqns. 4 and 5) *vs.* electrical field strength for different capillary diameters. For numerical values used in the calculations, see Table I.

and Table II, as follows. (1) The minima of the *H–E* curves are located at very high field strengths, far above the currently used values of 30–40 kV m^{-1}. Such high field strengths can only be used in practice if the Joule heat generated can be efficiently removed. (2) For analyses that do not require high plate numbers, very short analysis times can be realized. Owing to the physical dimensions of the currently used instruments, the short column lengths needed (*e.g.*, 0.5 cm for 10 000 plates on a 100-μm column) cannot be used. (3) The maximum allowable detector volume increases with plate number and decreases with column diameter. Detector volumes of the order of 100 pl need to be realized to

TABLE I

TYPICAL VALUES OF PHYSICAL QUANTITIES USED IN THE CALCULATIONS

Symbol	Quantity	Unit	Value
c	Molar concentration	$mol\ m^{-3}$	10
D_m	Diffusivity	$m^2\ s^{-1}$	10^{-9}
K	Thermal conductivity	$W\ m^{-1}\ K^{-1}$	0.4
γ	Tortuosity factor	–	0.6
ϵ	Void fraction	–	0.75
ε_0	Permittivity of free space	$C^2\ N^{-1}\ m^{-2}$	$8.85 \cdot 10^{-12}$
ε_r	Relative permittivity	–	80
η	Viscosity	$N\ s\ m^{-2}$	10^{-3}
ζ	Zeta potential	V	$5 \cdot 10^{-2}$
κ	Profile factor	–	6
λ	Equivalent conductivity	$m^{-2}\ mol^{-1}\ \Omega^{-1}$	0.015

TABLE II

CHARACTERISTIC PARAMETERS FOR TWO COLUMN DIAMETERS: 100 μm (H_{min} = 0.49 μm, E_{opt} = 84 kV m^{-1}) AND 50 μm (H_{min} = 0.24 μm, E_{opt} = 168 kV m^{-1})

d_c (μm)	N	t_E (s)	t_A (min)	$\sigma_{V,0}$ (pl)	V_{DET} (pl)
100	10 000	1.6	0.3	290	250
	50 000	8	1.5	640	550
	100 000	16	3.0	900	770
	500 000	80	15	2030	1760
	1 000 000	160	30	2900	2470
50	10 000	0.4	0.07	40	35
	50 000	2.0	0.37	80	70
	100 000	4.1	0.75	110	100
	500 000	20	3.7	250	210
	1 000 000	40	7.5	360	310

exploit fully the advantages of electro-drive separations.

Our integrated design for electrically driven separations aims at meeting the requirements set by the above three conclusions.

EXPERIMENTAL

Instrument design

In Fig. 2 a schematic diagram of the integrated instrument is shown. As can be seen, the injector, column and detector are all located within the same thermostated enclosure. The enclosure, in fact, is intended to be a small cartridge. The necessity for active thermostating can be appreciated if one bears in mind that electrophoretic and electroosmotic mobilities, and hence retention times, vary by about 2% K^{-1}. Also, because the optics of the fluorescence detector and also the buffer and sample vials are remote from the actual instrument, the length of the separation capillary can be very short (several millimetres). The design depicted in Fig. 2 is only possible by directly connecting optical fibres and injection capillaries to the separation capillary, *i.e.*, without employing bulky connecting devices. Direct connection is obtained by the use of a carbon dioxide laser to machine bores in the wall of the separation capillary. In the injector design, capillaries are inserted in these bores and an injector similar to that reported by Verheggen *et al.* [15] is the result. Flow through either the injection or the separation capillary can be effected by the appropriate application of the voltage. In the design of the fluorescence detector cell, optical fibres are placed in the two bores, which are now at right-angles. In this paper, we focus on detector performance. A detailed description of the construction of the detector is given in the next section.

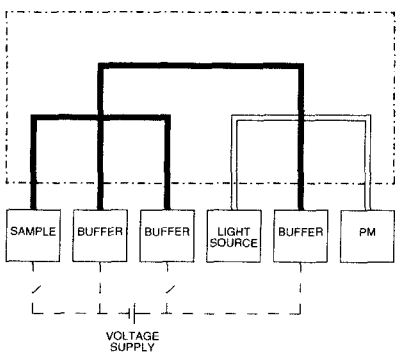

Fig. 2. Schematic diagram of integrated instrument design. The injector is on the left-hand side and the detector on the right-hand side. Heavy solid lines indicate fused-silica capillary, double lines optical fibres. Dashed lines are used for electrical connections. Note that the injector, column and detector are all within the same thermostated enclosure (dot-dashed lines). PM = Photomultiplier.

Detector cell construction

At the desired position of the cell, 2 cm of the protective, polyimide coating of the fused-silica capillary were removed. A carbon dioxide laser (Edinburgh Instruments, Edinburgh, UK) was used to make the bores in the walls of the capillaries [16]. The design is illustrated in Fig. 3. The diameter of the resulting bores depends on the outer and inner diameters of the capillary (330 and 100 μm, respectively), the power and duration of the laser shot (2.4 W and 400 ms, respectively) and the distance to the object (2.9 mm). Using the above conditions, tapered bores having a top diameter of 35 μm were obtained, centred with an accuracy of 2 μm.

To increase the light intensity in the cell and to decrease the fluorescent background due to fluorescing centres in the adhesive, the detector cell was coated with a silver mirror prior to the application of the adhesive. Silver films were vapour-deposited on the fused silica of the capillary. Vapour deposition was performed in an HV system (Balzers, Liechtenstein) using an Airco-Temescal E-gun at a rate of 0.3

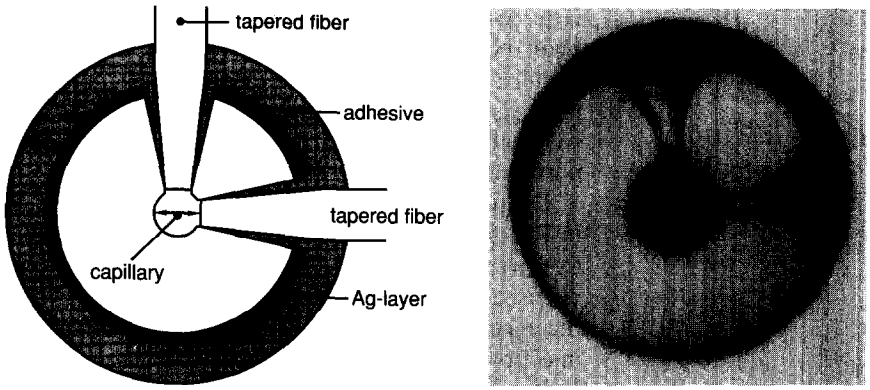

Fig. 3. Fluorescence detector design. A drawing of the cell is shown on the left-hand side and an optical micrograph of the cell (no optical fibres connected) on the right-hand side.

nm s^{-1}. The thickness of the silver layer was 30 nm.

Spectraguide optical fibres with high UV transmission were obtained from Spectrum (Sturbridge, MA, USA). The 100-μm core of the fibres was tapered to 35 μm in order to fit snugly into the bores in the capillary walls. The metal-coated capillary and the optical fibres were joined with a two-component epoxy adhesive (Bison, Middelburg, Netherlands).

Assuming a cylinder with a length of 100 μm and a diameter of 35 μm, the illuminated volume of the detector cell described above is 96 pl.

Experimental set-up

In all experiments, a continuous laser was employed (Model 4210 NB, Liconix, Santa Clara, CA, USA). The 442-nm emission line of the He–Cd laser was used, having an energy of *ca.* 10 mW. The laser was focused on one of the fibres of the detector cell using a lens (f = 125 mm). The output from the other fiber was fed to a Model 150UVP photomultiplier (Philips, Eindhoven, Netherlands). The laser-induced fluorescence was measured with a 530-nm short-wavelength cut-off filter in front of the photomultiplier. The signal of the photomultiplier was recorded via a Model 160 boxcar (Princeton Applied Research, Princeton, NJ, USA), using a static gate, with either an x–t recorder or a Model 10B computing integrator (Milton Roy, Riviera Beach, FL, USA).

In all experiments, a Model DA-30 stabilized, high-voltage (0–30 kV) power supply (Spectrovision, Chelmsford, MA, USA) was used.

Procedures

All experiments were performed using phosphate buffers adjusted to the desired pH by titration with phosphoric acid. The test solutes were obtained from various sources and were all of the highest purity available. High-purity deionized water was used to make up the solutions. Samples were introduced into the capillary using electromigration. In determining the calibration graph and the detection limit for fluorescein, concentration fronts were injected and the heights of the resulting blocks were measured. Noise levels were measured by recording the baseline over 1-min intervals and taking the average of six measurements of the peak-to-peak signal as $4\sigma_N$ [17]. Electrophoretic separations were performed by injecting the sample mixture at a voltage of 3 kV for 3 s.

RESULTS AND DISCUSSION

In Fig. 4, a calibration graph for fluorescein is shown. Over the three orders of magnitude investigated, good linearity is observed. From the slope of the plot and the noise (see Experimental), the concentration detection limit is determined to be $2 \cdot 10^{-9}$ M of fluorescein. Using an illuminated volume of 100 pl, this corresponds to $2 \cdot 10^{-19}$ moles (200 zmol) in the detector cell.

Owing to the great variety of experimental systems and test solutes used, a direct comparison with literature data on laser-induced fluorescence detection is not straightforward. The concentration detection limit quoted above compares well with

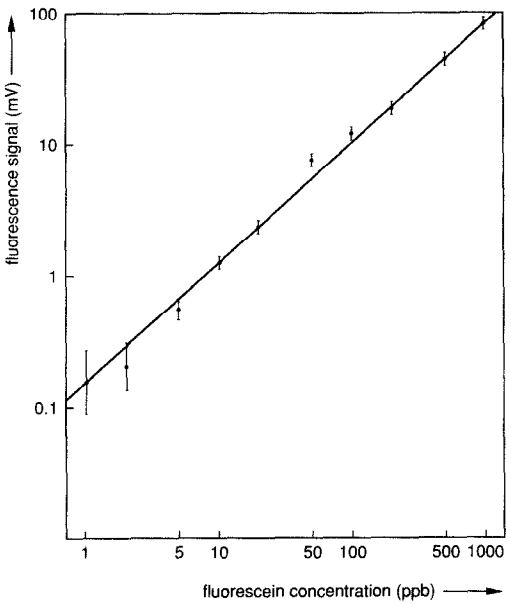

Fig. 4. Calibration graph for fluorescein, obtained using the detector cell in Fig. 3.

earlier values for highly fluorescing compounds using on-column detection [17,18]. Substantially lower detection limits were reported by Folestad *et al.* [19] ($5 \cdot 10^{-14}$ *M* fluoranthene). However, they used a free-falling jet cell that requires flow-rates far higher than can be attained in electrically driven systems. In CZE very impressive results were obtained by Dovichi and co-workers [20,21] using a sheath flow cuvette [$5 \cdot 10^{-12}$ *M* of (derivatized) alanine] and by Sweedler *et al.* [22] using axial illumination and a charge coupled device (CCD) readout ($1 \cdot 10^{-12}$ *M* of fluorescein isothiocyanate). Again, we encounter a compatibility problem. It is not easy to see how either the sheath flow cuvette or axial illumination can be combined with short column lengths and integral thermostating that are necessary to achieve the high efficiencies and separation speeds. In our integrated design, such a compatibility problem does not exist. In addition, we feel that there is ample room for improving the detection limit of our detector cell. As the standard deviation of the background signal is now limiting its performance, increasing the laser power will not be beneficial. Rather, we should either try to decrease the background itself by improving on the optics or to decrease its variance. Several ways to achieve the latter can be envisaged. One could either contemplate the use of a commercially available laser power stabilizer (Liconix) or build a double-beam instrument in which fluctuations are corrected for by subtracting or ratioing the "blank" and "sample" photocurrents.

The possibility of fast separations is demonstrated in Fig. 5, which shows the separation of four laser dyes within 35 s using a 4-cm capillary. In this work, we used traditional electromigration (3 s, 3 kV) as the injection technique. It is clear that this method of injection has an adverse effect on the separation. Using an electroosmotic mobility of $7.8 \cdot 10^{-8}$ m^2 $V^{-1}s^{-1}$ (determined using the technique described by Huang *et al.* [23]), the volume injected is calculated to be 17 nl. Assuming an injection profile factor of 6, the peak width at half-height due to the injection is 0.95 s. Comparing this result with the electropherogram in Fig. 5, it is seen that the width of the peak travelling at the electroosmotic velocity (approximately the first peak) is completely dominated by the contribution of the injection. In practice, the consequence of the large contribution of the injection is that we cannot use the desirable high field strengths without serious resolution losses. Note that the field strength used to obtain the electropherogram in Fig. 6 is much lower than the optimum values quoted in the Theory section. Obviously, injection devices that allow for smaller

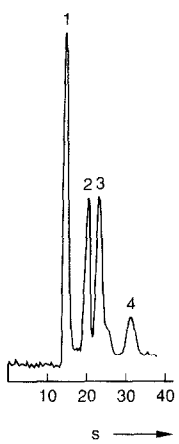

Fig. 5. Electropherogram of the separation of four laser dyes. Conditions: field strength, 33 kV m^{-1}; buffer, 2 m*M* phosphate (pH 6); capillary, 4.0 cm × 100 μm I.D.; temperature, ambient; injection, 3 s at 3 kV. Sample: (1) 7 ppm rhodamine B; (2) 7 ppm sulphorhodamine B; (3) 0.4 ppm fluorescein; (1) 17 ppm 4',5'-diiodofluorescein.

injection volumes than electromigration are necessary to realize the very short analysis times offered by short column lengths. We feel that the injector described in the first paragraph under Experimental, with which injection volumes of the order 100 pl are possible, can serve the purpose.

CONCLUSIONS

An integrated instrument for electrically driven separations has been designed. The design facilitates the use of short columns and high field strengths, so that high resolutions and short analysis times can be attained. The detector cell has the required small volume (100 pl) and allows $2 \cdot 10^{-19}$ mol of fluorescein to be detected. In combination with a short capillary (4 cm), four laser dyes could be separated within 35 s.

The separation speed is currently limited by the injection technique used (electromigration at 3 kV for 3 s). To decrease the contribution of the injection to the total peak width, the injected volume has to be reduced. This may be achieved using the injector of the proposed instrument.

REFERENCES

1 F. E. P. Mikkers, F. M. Everaerts and Th. P. E. M. Verheggen, *J. Chromatogr.*, 169 (1979) 11.
2 J. W. Jorgenson and K. D. Lukacs, *J. Chromatogr.*, 218 (1981) 209.
3 J. W. Jorgenson and K. D. Lukacs, *Anal. Chem.*, 53 (1981) 1298.
4 S. Terabe, K. Otsuka, K. Ishikawa, A. Tsuchiya and T. Ando, *Anal. Chem.*, 56 (1984) 111.
5 S. Terabe, *Trends Anal. Chem.*, 8 (1989) 129.
6 T. Tsuda, K. Nomura and G. Nakagawa, *J. Chromatogr.*, 99 (1982) 248.
7 J. H. Knox and I. H. Grant, *Chromatographia*, 24 (1987) 135.
8 R. T. Kennedy, M. D. Oates, B. R. Cooper, B. Nickerson and J. W. Jorgenson, *Science*, 246 (1989) 57.
9 P. K. de Bokx, P. C. Baarslag and H. P. Urback, *Sep. Sci. Technol.*, in press.
10 P. J. Schoenmakers, *The Optimization of Chromatographic Selectivity. A Guide to Method Development*, Elsevier, Amsterdam, 1986.
11 P. J. Naish, C. V. Perkins and D. P. Goulder, *Chromatographia*, 20 (1985) 335.
12 J. C. Sternberg, *Adv. Chromatogr.*, 2 (1966) 205.
13 C. L. Rice and R. Whitehead, *J. Phys. Chem.*, 69 (1965) 4017.
14 F. Foret, M. Deml and P. Boček, *J. Chromatogr.*, 452 (1988) 601.
15 Th. P. E. M. Verheggen, J. L. Beckers and F. M. Everaerts, *J. Chromatogr.*, 452 (1988) 615.
16 X. Huang, T.-K. J. Pang, M. J. Gordon and R. N. Zare, *Anal. Chem.*, 59 (1987) 2747.
17 H. P. M. van Vliet and H. Poppe, *J. Chromatogr.*, 346 (1985) 149.
18 E. J. Guthrie, J. W. Jorgenson and P. L. Dluzneski, *J. Chromatogr. Sci.*, 22 (1984) 171.
19 S. Folestad, L. Johnson, B. Josefsson and B. Galle, *Anal. Chem.*, 54 (1982) 925.
20 Y.-F. Cheng and N. J. Dovichi, *Science*, 242 (1988) 562.
21 S. Wu and N. J. Dovichi, *J. Chromatogr.*, 480 (1989) 141.
22 J. V. Sweedler, J. B. Shear, H. A. Fishman, R. N. Zare and R. H. Scheller, *Anal. Chem.*, 63 (1991) 496.
23 X. Huang, M. J. Gordon and R. N. Zare, *Anal. Chem.*, 60 (1988) 1837.